Charge Transport and Dipolar Relaxations in Hyperbranched Polyamide Amines

J. R. Sangoro,*,† G. Turky,‡ M. Abdel Rehim,§ C. Iacob,† S. Naumov,† A. Ghoneim, J. Kärger,† and F. Kremer†

Institute of Experimental Physics I, University of Leipzig, Leipzig, Germany; Microwave Physics and Dielectrics Department, NRC, Cairo, Egypt; and Packing and Packaging Department, NRC, Cairo, Egypt

Received October 27, 2008; Revised Manuscript Received January 26, 2009

ABSTRACT: Broadband dielectric spectroscopy, pulsed field gradient nuclear magnetic resonance (PFG NMR), and differential scanning calorimetry are combined to study charge transport and dipolar relaxations in novel hyperbranched polyamide amines. The dielectric spectra are dominated by conductivity contributions at higher temperatures (masking out the structural α-relaxation process), whereas two secondary dipolar relaxation processes are observed at lower temperatures for the two samples investigated. Based on Einstein and Einstein−Smoluchowski relations, the diffusion coefficient is extracted from the dielectric spectra—in quantitative agreement with independent PFG NMR measurements. It exhibits a Vogel−Fulcher−Tammann temperature dependence, while the effective number density of the charge carriers varies only weakly with temperature. Charge transport and structural α-relaxation are found to be characterized by a decoupling index of ∼7 for the hyperbranched polymers studied.

Introduction

All dendritic polymers including dendrimers and hyperbranched polymers (HBPs) have treelike structures. They possess a highly branched backbone, which gives access to a large number of reactive groups. Their structure gives them excellent flow and processing properties, which have attracted a great deal of attention for many applications in coatings and formulations, e.g., powder coatings, high solid coatings, flame-retardant coatings, and barrier coatings for flexible packaging.[1−8] In recent years these materials have shown promise in fields of the development of vaccines, antiviral, antibacterial, and anticancer therapeutics. A comparison of the features of dendrimers with those of linear polymers shows that the architecture of the dendrimers can provide several advantages for drug delivery applications. For example, the controlled multivalency of dendrimers can be used to attach several drug molecules, targeting groups and solubilizing groups to the periphery of the dendrimers in a well-defined manner. In addition, the low polydispersity of dendrimers should provide reproducible pharmacokinetic behavior, in contrast to that of some linear polymers containing fractions with vastly different molecular weight within a given sample. Furthermore, the globular shape of dendrimers, as opposed to the random coil structure of most linear polymers, could affect their biological properties. Because polymers have shown great potential in the development on anticancer drug delivery systems, the applications of dendritics in this area is particularly promising.[9,10]

Hyperbranched polymers are often prepared by a one-pot polymerization of AB_x-type monomers in a method known as single monomer methodology or by direct polymerization of two suitable monomers to attain a highly irregular structure. These polymers are composed of terminal, linear, and dendritic units that are distinguished by the number of unreacted functional groups in the unit. The degree of branching (DB) is largely used as a parameter to indicate the architecture of hyperbranched polymers and is defined as $DB = (D + T)/(D + T + L)$, where D is the number of dendiritic units, T is the number of terminal units, and L is the number of linear units. High functional group densities which are easily tailored by changing the nature of the end groups have provided various creative materials design.[11] Thus, the resulting HBPs are expected to be produced in large quantities at commercially feasible costs.[12]

Broadband dielectric spectroscopy (BDS)[13,14] is a fruitful technique for investigating the dynamics of HBPs in bulk[15−17] or as thin films.[18,19] In their study of hyperbranched polyesters with hydroxyl units as the terminal groups, Malmstroem et al. found three relaxations: γ and β below the calorimetric glass transition temperature (subglass processes) and one associated with the glass transition (α-process) for the fifth generation.[20] The dependence of conductivity on the generation number has been reported.[21] The conductivity contribution has been found to mask out the structural α-relaxation process in many HBPs. Similarly, it has been shown that the dielectric spectra of higher generations of dendrimers are dominated by charge transport.[22] However, experimental and theoretical effort in this field has been focused on developing new synthesis techniques at the expense of physical characterization of the dendritic and hyperbranched macromolecules. In addition, the mechanisms of charge transport in these materials are not well understood.

In the current paper dielectric properties of hyperbranched polyamide amines are investigated by combining BDS, pulsed field gradient nuclear magnetic resonance (PFG NMR), and differential scanning calorimetry (DSC). Charge transport and dipolar relaxations in these novel materials are explored in detail.

Experimental Section

Diethylenetriamine (99%), ethylenediamine (ED, 98%), and methanol (99.9%) were purchased from Aldrich Chemicals Co., and methyl acrylate (MA, >99%) was obtained from BDH Chemicals Co. and used for synthesis of hyperbranched polymers without further purification. The preparation of hyperbranched polyamide amine, abbreviated in the text with respect to the nitrogen content as PAMAM 1 for lower and PAMAM 2 for higher nitrogen content, was made in accordance with Liu et al.[23] The method was

* To whom correspondence should be addressed.
† University of Leipzig.
‡ Microwave Physics and Dielectrics Department, NRC.
§ Packing and Packaging Department, NRC.

10.1021/ma8024046 CCC: $40.75
Published on Web 02/17/2009

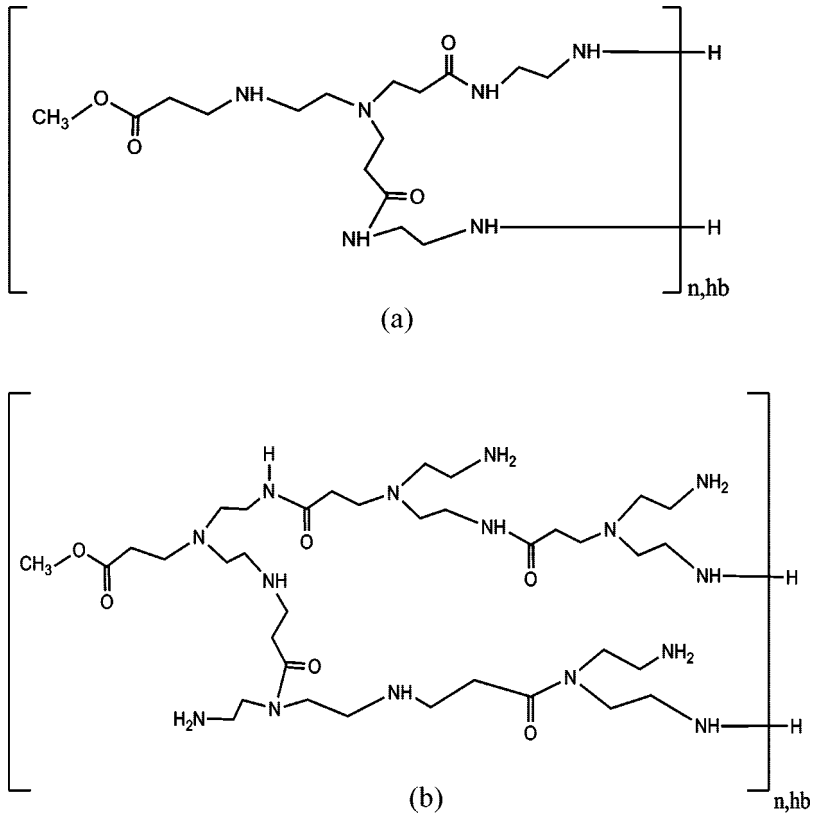

Figure 1. Chemical structure of polyamide amines (a) PAMAM 1 and (b) PAMAM 2 prepared by polycondensation of methyl acrylate and either ethylenediamine or diethylenetriamine.

carried out as follows: MA was added dropwise to the amine/methanol solution (feed ratio 1:1). The reaction mixture was kept at room temperature for 24−48 h. Methanol was removed from the reaction system under reduced pressure at 60 °C on a rotary evaporator. Under vigorous revolving and vacuum distillation, the mixture was kept at 60 °C for 1 h, 100 °C for 2 h, 110 °C for 2−4 h, and finally 135−150 °C for 2−4 h. The yellow viscous solid hyperbranched polymer is produced. Two different polymers were synthesized: the first was based on ethylenediamine (ED), which is poly(amidoamine) 1 (PAMAM 1), and the second, poly(amidoamine) 2 (PAMAM 2), was based on diethylenetriamine (DETA).

The Michael addition of the amine to MA yields an intermediate which is further self-condensed to give rise to PAMAM 1 and PAMAM 2 whose chemical structures are shown in parts a and b of Figure 1, respectively. In both cases, two types of linear groups are formed within the polymer structure though the structure of PAMAM 2 is the more complex of the two. Also, nitrogen content in the PAMAM 2 is more than that prepared using ED as was confirmed by elemental analysis. The resulting polymers have amido and tertiary amino units in their backbones and many primary amino groups in their terminal chains. The polymers showed good solubility in water and in polar solvents and were synthesized without using catalysts, thereby enhancing their purity.

^{1}H NMR spectra were obtained from a Varian Mercury-Oxford-300 MZ using DMSO-d_6 as the main solvent for the two samples (for PAMAM 1: ^{1}H NMR (DMSO-d_6): δ = 1.80−2.3 (NH_2, NH), 2.3−2.5 ($COCH_2$), 2.5−3.0 [$COCH_2CH_2NH$, $NH(CH_2)_2NH$, $NH(CH_2)_2$. 3.2−3.50 (NCH_2), 3.5−4.0 (CH_3O) and for PAMAM 2: ^{1}H NMR (DMSO-d_6): δ = 2.16−2.4 (NH_2, NH), 2.4−2.96 ($COCH_2$, $NHCH_2$, NH_2CH_2), 3.16−3.52 (NCH_2), 3.56−3.68 (CH_3O); the molar mass of both samples is 2000 g/mol). The molecular weights and the polydispersities were measured using gel permeation chromatography (GPC) through Zorbax PSM 60 + 300 column coupled with differential refractometer. As eluent, a mixture of dimethylacetamide, 2 vol % of water, and 3 g/L of LiCl was used with flow rate of 0.5 mL min^{-1}. Linear polyvinylpyridine (PVP) standard was used to calibrate the column. Thermogravimetric analysis (TGA) was carried out using a TGA Q 5000 (TA Instruments), heating program 40−700 °C, and the heating rate 10 °C/min. These measurements showed weight loss at about 105 °C. This could be considered to be due to the water content which was about 3.7% for PAMAM 1 and 4% for PAMAM 2. DSC measurements were carried out by using a differential scanning calorimeter Q 1000 TA at scan rate of 10 K/min. The calorimetric glass transition temperature was found to be 259.8 K for PAMAM 1 and 234.8 K for PAMAM 2.

The dielectric measurements were performed between 0.01 Hz and 10 MHz using a Solatron 1260 impedance analyzer (0.1 Hz −0.1 MHz) and a Novocontrol high-resolution alpha analyzer (0.01 Hz−10 MHz). The analyzers were assisted by a Quatro temperature controller using pure nitrogen as heating agent and assuring a temperature stability better than 0.2 K. The samples were pressed at 330 K between two gold-plated stainless steel electrodes of 20 mm in diameter. Fused-silica fibers with a diameter of 50 μm were used as spacers. The samples were annealed at temperatures above the calorimetric glass transition temperatures (more precisely, at 380 K) in vacuum for 12 h prior to performing dielectric measurements. The dielectric spectra coincide for both the heating and cooling scans, indicating thermal stability of the samples. On the other hand, PFG NMR was used as a tool for studying translational diffusion. In this method the attenuation of the echo signal from Hahn spin-echo pulse sequence containing a magnetic field gradient pulse in each period was used to measure the displacement of the observed spins. PFG NMR was used to obtain translational diffusion coefficients in accordance with suggestions of Annat et al.[24] All the measurements were done in a dry nitrogen atmosphere.

Results and Discussion

The equivalence of the complex dielectric function ε^* ($= \varepsilon' - i\varepsilon$) and complex conductivity function σ^* ($= \sigma' + i\sigma$) can be given as $\sigma^*(\omega,T) = i\varepsilon_0\omega\varepsilon^*(\omega,T)$, implying that $\sigma' = \varepsilon_0\omega\varepsilon''$ and $\sigma'' = \varepsilon_0\omega\varepsilon'$ (ε_0 being the vacuum permittivity). The dielectric spectra of PAMAM 1 measured between 0.1 Hz and

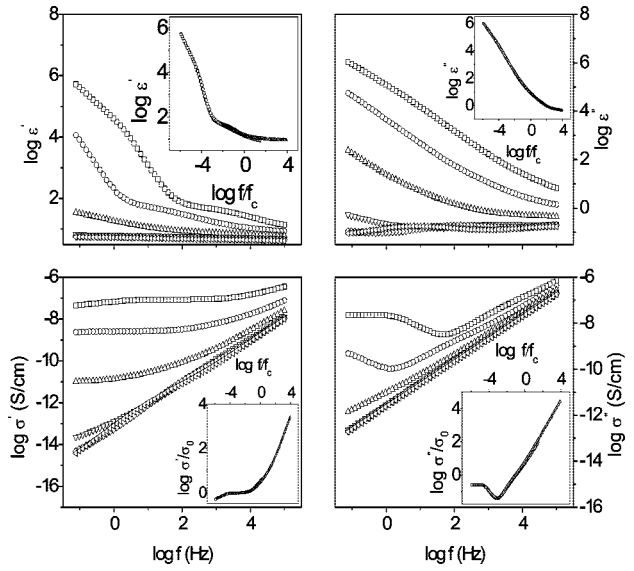

Figure 2. Complex dielectric function $\varepsilon^* (= \varepsilon' - i\varepsilon)$ and complex conductivity function $\sigma^* (= \sigma' + i\sigma)$ of PAMAM 1 as a function of frequency at different temperatures (□, 313.15 K; ○, 293.15 K; △, 273.15 K; ▽, 253.15 K; right-tilted △, 233.15 K; left-tilted △, 203.15 K). Inset: scaling with respect to the characteristic frequency, f_c, and dc conductivity, σ_0, for different temperatures. The error bars are comparable to the size of the symbols, if not specified otherwise.

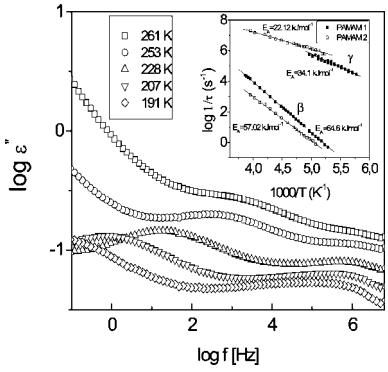

Figure 3. Imaginary part of the complex dielectric function versus frequency at different temperatures illustrating the secondary relaxation processes in PAMAM 2 sample. Inset: Arrhenius-type temperature dependence of the secondary relaxation rates ($1/\tau$) of both polymers at lower temperatures (191−261 K). The values of activation energies are indicated. Unless specified otherwise, the logarithm is to base 10.

0.1 MHz as a function of temperature are shown in Figure 2 in plots of ε', ε'', σ', and σ'' versus frequency. It is instructive to present the dielectric spectra in terms of both complex functions since they emphasize different aspects of the dielectric processes under study. In the inset of Figure 2 the experimental spectra are scaled with respect to the dc conductivity and the characteristic frequency at which the real part of the conductivity begins to increase with frequency. Coinciding plots are obtained (after subtraction of the contribution of secondary dipolar relaxations at lower temperatures) in agreement with many ion-conducting glass-forming liquids and glasses.[25−29]

Figure 3 shows the dielectric loss, $\varepsilon(\omega,T)$, of PAMAM 2 (in the lower temperature range between 190 and 260 K). Two relaxation peaks γ and β can be observed at temperatures lower than the T_g. The γ-relaxation is attributed to fluctuation of the focal group (methoxy group). Its intensity is comparable to that of the β-process. The dielectric spectra of the secondary relaxations were fitted using the empirical Havriliak−Negami (HN) function expressed as

$$\varepsilon^*_{HN} = \varepsilon_\infty + \frac{\Delta\varepsilon}{(1 + (i\omega\tau_{HN})^\beta)^\gamma} \quad (1)$$

where $\Delta\varepsilon$ is the dielectric strength, ε_∞ is the relaxed value of ε', τ_{HN} is the Havriliak−Negami relaxation time (related to the α-relaxation time), and β and γ are shape parameters.

The temperature dependence of all the secondary relaxations is analyzed by means of the Arrhenius equation given by

$$\log(\upsilon_p) = \log \nu_\infty - \frac{\ln 10 E_A}{k_B T} \quad (2)$$

as shown in the inset of Figure 3 where E_A is the activation energy, ν_p the frequency of maximal loss (relaxation rate) of the relaxation process under consideration, k_B the Boltzmann constant, and υ_∞ the relaxation rate in the high temperature limit. The activation energy of the γ-process was found to be 34 kJ/mol for PAMAM 1 and 22 kJ/mol for PAMAM 2. The β-relaxation observed at lower frequencies is related to the amino groups. This group is found in three structural forms: terminal, linear, and dendritic. This may explain the broadness of the observed peaks. The apparent activation energies for these dynamic processes are 64 and 57 kJ/mol, respectively. These values of the activation energies indicate that the corresponding relaxations are associated with local movements. With increasing temperature the peak of the β-relaxation becomes broader.

In recent papers, we have combined Einstein and Einstein−Smoluchowski relations to extract diffusion coefficients of charge carriers from the measured dielectric spectra in quantitative agreement with independent PFG NMR measurements.[30,31] The dc conductivity σ_0 is given by

$$\sigma_0 = nq\mu = \frac{nq^2}{kT}D = \frac{nq^2}{kT}\frac{\lambda^2\omega_c}{6} \quad (3)$$

where λ denotes the characteristic hopping distance, q is the elementary charge, n is the effective number density of charge carriers, k is Boltzmann's constant, D is the diffusion coefficient, μ is mobility, and ω_c is the characteristic hopping rate of the charge carriers. By taking the hopping distance values comparable to the Pauling diameter,[32] i.e., $\lambda = 0.2$ nm, the diffusion coefficients are readily determined. Within this framework charge transport is accomplished by hopping of charge carriers. It is worth mentioning that the characteristic hopping rate (ω_c) in the materials reported in the current work is approximately equivalent to the attempt rate (ω_e) to overcome the dc limiting barriers within the random barrier model developed by Dyre.[33,34]

Figure 4 shows the diffusion coefficients obtained from dielectric measurements and PFG NMR. The corresponding temperature dependence of mobilities is also presented as well as the effective number density of the charge carriers. The Barton−Nakajima−Namikawa (BNN) relation $\sigma_0 \sim \omega_c$ (inset, Figure 4a) holds for the materials under study. The temperature dependence of the mobility μ (and consequently diffusion coefficient) can be approximated by the empirical Vogel−Fulcher−Tamman (VFT) equation[11]

$$\mu(T) = \mu_\infty \exp\left[\frac{-D_f T_0}{T - T_0}\right] \quad (4)$$

where μ_∞ is mobility in the high temperature limit, D_f is a constant (often referred to as fragility parameter), and T_0 denotes the Vogel temperature. This delivers $\mu_\infty = (5.0 \pm 0.5) \times 10^{-8}$ m^2 V^{-1} s^{-1}, $D_f = 16.8 \pm 0.5$, and $T_0 = 167 \pm 2$ K for PAMAM 1 and $\mu_\infty = (2.7 \pm 0.4) \times 10^{-7}$ m^2 V^{-1} s^{-1}, $D_f = 16.2 \pm 0.6$, and $T_0 = 172 \pm 3$ K for PAMAM 2. The obtained fit parameters apply for both the dielectric and PFG NMR data despite the

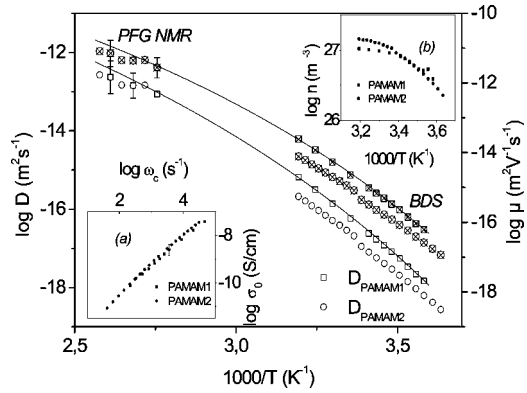

Figure 4. Diffusion coefficient determined by the Einstein and Einstein−Smoluchowski equation[30,31] (using ω_c as hopping rate and $\lambda = 0.2$ nm as hopping distance) compared with the diffusion coefficient measured by PFG NMR. Additionally, the mobility of the charge carriers is determined by Einstein relation (symbols filled in with crosses). Inset: (a) dc conductivity, σ_0, versus the characteristic radial frequency, ω_c (BNN plot), and (b) effective number of charge carriers as a function of inverse temperature.

difference in the time scales of the two techniques in the current measurement.

In order to understand the dominating mechanisms of charge transport in amorphous materials further, the decoupling index, R_τ, which is defined as the ratio of the structural relaxation time to the conductivity relaxation time has been suggested by Angell.[35,36] This can often reach very large numbers and is best described in logarithmic representation. It has been empirically expressed as decoupling index (log) = 14.3 + log $\sigma_0(T_g)$. T_g values obtained from DSC measurements for the polymer samples are −13.2 and −38.2 °C for PAMAM1 and PAMAM2, respectively. The Vogel−Fulcher−Tammann (VFT) equation is used to extrapolate the measured dc conductivity to the temperatures corresponding to the calorimetric glass transition temperatures. A decoupling index ∼7 is obtained for the systems under study, indicating that charge transport is dominated by ionic species that are 7 orders of magnitude more mobile than would be expected from structural relaxation. Such high decoupling indices have been attributed to proton conduction.[36]

Studies on hyperbranched polymers in which both the dipolar relaxations and charge transport are investigated in detail are scarce. Whereas the modulus formalism is sometimes adopted for analyzing charge transport in such systems, the approach is not generally accepted in the scientific community. It should be mentioned that the characteristic electrical relaxation rate from the aforementioned formalism is approximately equal to the characteristic diffusion rate discussed in the current work.

Conclusion

For the first time mass and charge transport are measured for hyperbranched polyamide amines by combining pulsed field gradient NMR and broadband dielectric spectroscopy. Both methods agree well with each other delivering for the diffusion coefficient and hence the electrical mobility a VFT temperature dependence, while for the number density of charge carriers an Arrhenius-type thermal activation is found. A refined analysis suggests that the primary mechanism of charge transport is due to proton conduction, a result which is supported as well by the decoupling index obtained.

Acknowledgment. Financial support from the Deutsche Forschungsgemeinschaft under the DFG SPP 1191 Priority Program on Ionic Liquids is gratefully acknowledged.

References and Notes

(1) Jikei, M.; Kakimoto, M. *Prog. Polym. Sci.* **2001**, *26*, 1233.
(2) Voit, B. I. *J. Polym. Sci., Part A: Polym. Chem.* **2000**, *38*, 2505.
(3) Froehling, P. *J. Polym. Sci., Part A: Polym. Chem.* **2004**, *42*, 3110.
(4) Hult, A., Johansson, M., Malmstroem, E., Roovers J., Eds.; *Advances in Polymer Science*; Springer-Verlag: Berlin, 1999; Vol. *143*, p 1.
(5) Diao, P.; Guo, M.; Hou, Q.; Xiang, M.; Zhang, Q. *J. Phys. Chem. B* **2006**, *110*, 20386.
(6) Whiting, G. L.; Snaith, H. J.; Khodabakhsh, S.; Andreasen, J. W.; Breiby, D. W.; Nielsen, M. M.; Greenham, N. C.; Friend, R. H.; Huck, W. T. S. *Nano Lett.* **2006**, *6*, 573.
(7) Xu, J.; Qiu, F.; Zhang, H.; Yang, Y. *J. Polym. Sci., Part B: Polym. Phys.* **2006**, *44*, 2811.
(8) Di Gianni, A.; Trabelsi, S.; Rizza, G.; Sangermano, M.; Althues, H.; Kaskel, S.; Voit, B. *Macromol. Chem. Phys.* **2007**, *208*, 76.
(9) Duncan, R.; Izzo, L. *Adv. Drug Delivery Rev.* **2005**, *57*, 2215.
(10) Stiriba, S.-E.; Frey, H.; Haag, R. *Angew. Chem., Int. Ed.* **2002**, *41*, 1329.
(11) Kim, Y. H.; Webster, O. W. *Macromolecules* **1992**, *25*, 5561.
(12) Malmstroem, F.; Hult, A. *Macromolecules* **1996**, *29*, 1222.
(13) Kremer, F.; Schönhals, A. *Broadband Dielectric Spectroscopy*; Springer: Berlin, 2003.
(14) Riande, E.; Diaz-Calleja, R. *Electrical Properties of Polymers*; Marcel Dekker: New York, 2004.
(15) Czech, P.; Okrasa, L.; Ulanski, J.; Bioteux, G.; Mechin, F.; Cassgnau, Ph *J. Appl. Polym. Sci.* **2007**, *105*, 89.
(16) Garcia-Bernabe′, A.; Diaz-Calleja, R.; Haag, R. *Macromol. Chem. Phys.* **2006**, *207*, 970.
(17) Garcia-Bernabe′, A.; Dominguez-Espinosa, G.; Diaz-Calleja, R.; Riande, E.; Haag, R. *J. Chem. Phys.* **2007**, *127*, 124904.
(18) Serghei, A.; Mikhailova, Y.; Huth, H.; Schick, C.; Eichhorn, K.-J.; Voit, B.; Kremer, F. *Eur. Phys. J. E* **2005**, *17*, 199.
(19) Serghei, A.; Mikhailova, Y.; Eichhorn, K.-J.; Voit, B.; Kremer, F. *J. Polym. Sci., Part B: Polym. Phys.* **2006**, *44*, 3006.
(20) Malmstroem, E.; Liu, F.; Boyd, R. H.; Hult, A.; Gedde, U. W. *Polym. Bull.* **1994**, *32*, 679.
(21) Zhu, P. W.; Zheng, Sh.; Simon, G. *Macromol. Chem. Phys.* **2001**, *202*, 3008.
(22) Mijovic, J.; Ristic, S.; Kenny, J. *Macromolecules* **2007**, *40*, 5212.
(23) Liu, C.; Gao, C.; Yan, D. *Chem. Res. Chin. Univ.* **2005**, *21*, 345.
(24) Annat, G.; MacFarlane, D. R.; Forsyth, M. *J. Phys. Chem. B* **2007**, *111*, 9018.
(25) Roling, B.; Happe, A.; Funke, K.; Ingram, M. D. *Phys. Rev. Lett.* **1997**, *78*, 2160.
(26) Sidebottom, D. L. *Phys. Rev. Lett.* **1999**, *82*, 3653.
(27) Zielniok, D.; Eckert, H.; Cramer, C. *Phys. Rev. Lett.* **2008**, *100*, 035901.
(28) Namikawa, H. *J. Non-Cryst. Solids* **1975**, *18*, 173.
(29) Iacob, C.; Sangoro, J. R.; et al. *J. Chem. Phys.* **2008**, *129*, 234511.
(30) Sangoro, J. R.; Serghei, A.; Naumov, S.; Galvosas, P.; Kärger, J.; Wespe, C.; Bordusa, F.; Kremer, F. *Phys. Rev. E* **2008**, *77*, 051202.
(31) Sangoro, J.; Iacob, C.; Serghei, A.; Naumov, S.; Galvosas, P.; Kärger, J.; Wespe, C.; Bordusa, F.; Stoppa, A.; Hunger, J.; Buchner, R.; Kremer, F. *J. Chem. Phys.* **2008**, *128*, 214509.
(32) Pauling, L. *The Nature of the Chemical Bond*, 3rd ed.; Cornell University Press: Ithaca, NY, 1960.
(33) Dyre, J. C. *J. Appl. Phys.* **1988**, *64*, 5.
(34) Dyre, J. C. *J. Phys. C: Solid State Phys.* **1986**, *19*, 5655.
(35) Angell, C. A. *Annu. Rev. Phys. Chem.* **1992**, *43*, 693.
(36) Mizuno, F.; Belieres, J.-P.; Kuwata, N.; Pradel, A.; Ribes, M.; Angell, C. A. *J. Non-Cryst. Solids* **2006**, *352*, 5147.

MA8024046